

1 Research Paper

2 **Pavement Rutting and Deformation Performance Analysis**
3 **through FEM**4 **Touqeer Ali Rind^{1*}, Muhammad Faarid Shah¹, Mohammad Ahmad¹, Hafiz Ahmed Waqas¹, Shiraz Ahmed¹ and**
5 **Asad Wahab¹**6 ¹ Department of Civil Engineering, Ghulam Ishaq Khan Institute of Engineering Sciences and Technology,
7 KPK, Pakistan. gcv2560@giki.edu.pk (M.F.S) ; gcv2567@giki.edu.pk (M.A) ; hafiz.waqas@giki.edu.pk
8 (H.A.W), shiraz.ahmed@giki.edu.pk (S.A), gcv2520@giki.edu.pk (A.W)9 * Correspondence Author: touqeer.ali@giki.edu.pk10 **Abstract**11 Rutting represents a severe, cumulative symptom of structural distress in flexible pave-
12 ments, which occurs due to the accumulation of permanent deformation when subjected
13 to repeated traffic loads and therefore adversely influences the quality of the ride, safety,
14 maintenance life and costs. This study assesses the influence of the pavement layer thick-
15 ness on the rutting depth using the three-dimensional finite element modeling (FEM) in
16 the ABAQUS computing program. The flexible pavement system was built as a detailed
17 numerical model with realistic material properties, nonlinear constitutive behavior and
18 repeated loading in a static situation. There were nine pavement designs which varied in
19 terms of the thickness of asphalt wearing course and base course, and evaluated stress
20 distribution and permanent deformation. The findings showed that adding the pavement
21 layer thickness has a significant effect on rutting depth, which is reduced due to the
22 spreading of loads and the strain concentrations, especially in the asphalt and subgrade
23 layers. On the other hand, thinner pavement layers had a greater deformation and they
24 experienced faster rates of rutting at the same loading conditions. The results offer useful
25 mechanistic information about the rutting behavior and contribute to the optimization of
26 layer thickness of pavements to increase durability, sustainability and long service per-
27 formance.28 **Keywords:** Flexible pavement, Rutting, Pavement layer thickness, Finite element model-
29 ing, ABAQUS, Permanent deformation.

30

31 **1. Introduction**32 Complex structural behavior during repeated and nonlinear loading conditions has
33 become a necessity to be explained by advanced numerical modeling. Studies using Finite
34 Element Method (FEM) have proven to be highly effective in stress transfer, material non-
35 linearities, and mechanisms of deformation in reinforced concrete and composite struc-
36 tures (Waqas et al., 2024; Mehran et al., 2024). The strength of FEM models has also been
37 confirmed by the usage of hybrid materials, nonlinear constitutive and performance pre-
38 diction under cyclic loading (Waqas et al., 2023; Amin et al., 2024). The recent studies also
39 emphasise the usefulness of FEM in determining the impact of geometry, reinforcement
40 arrangement, and material enhancement procedures on load-bearing capacity and long-

41 term performance (Waqas et al., 2023b). All these studies show that FEM can be trusted
42 as a simulation methodology when applied to sophisticated infrastructure systems and
43 that undergo repeated loading, especially when used in ABAQUS.

44 It is also true that flexible pavements are also subjected to millions of traffic load
45 cycles over their service life and therefore undergo progressive structural distress in
46 which rutting is one of the most significant distresses. Rutting comes in the form of per-
47 manent longitudinal depressions on the paths of the wheels and a considerable negative
48 influence on the quality of the ride, safety, and pavement serviceability (Du et al., 2018;
49 Hassani et al., 2020). Rutting development depends on a set of characteristics of traffic
50 loading, the thickness of pavement layers, the characteristics of the materials composing
51 the bound and unbound layers, and environmental factors, including temperature and
52 moisture (Singh and Sahoo, 2021; Luo and others, 2018). The traditional empirical and
53 mechanistic-empirical rutting models have been used to offer a background knowledge;
54 yet, due to their simplified assumptions, they do not represent properly the nonlinear,
55 time-dependent, and stress-dependent behavior of materials under a realistic field condi-
56 tion (Luo et al., 2017; Elseifi et al., 2018).

57 To overcome these shortcomings, pavement analysis using FEM has attracted much
58 interest because of its capacity to explicitly represent multi-layered pavement systems and
59 explicitly represent stress-strain behavior. The FEM of ABAQUS fully supports the three-
60 dimensional simulation of pavements with dynamic and repetitive loading by traffic and
61 permits a more realistic prediction of both rutting and permanent deformation (Nasr et
62 al., 2019; Wang and Wang, 2024). The platform supports the more advanced constitutive
63 models, such as viscoelasticity, viscoplasticity, creep and damage, which are critical in
64 simulating the recoverable and irrecoverable components of deformation in asphalt layers
65 and sub-grade soils (Hassani et al., 2020; Singh and Sahoo, 2021). The model fidelity is
66 also promoted with the correct representation of the layer interaction, tire-pavement con-
67 tact, and boundary conditions, which is essential in the development of rut depth
68 (Alnedawi et al., 2019; Du et al., 2018).

69 Two-dimensional and three-dimensional FEM methods have been used in the study
70 of pavements; the three-dimensional model offers better results in rutting morphology
71 and distributions of stresses across space, especially when the tire loading is non-uniform
72 (Elseifi et al., 2018; Su et al., 2023). mesh refinement plans and sub-modeling are primarily
73 used to find a compromise between the accuracy of the solution and the computational
74 efficiency (Wang et al., 2019; Singh and Sahoo, 2021). Wheel-tracking tests, repeated load
75 triaxial experiments, and accelerated pavement testing have shown great consistency be-
76 tween the rut depths as predicted by FEM and laboratory results (Elseifi et al., 2018;
77 Oditallah et al., 2025). However, there are still issues regarding simplified boundary con-
78 ditions, little field data over the long term, and not all thermal, hydraulic, and mechanical
79 coupling (Alnedawi et al., 2019; Luo et al., 2018).

80 The latest studies of FEM always identify that the rutting depth is extremely de-
81 pendent on pavement layer thickness, the magnitude of traffic loads, temperature, axle
82 arrangement, and subgrade stiffness. The thinner pavement layers have a greater strains
83 accumulation and rut development, and the greater the thickness of the layer, the better
84 the distribution of loads and the minimization of permanent deformity (Benakli et al.,
85 2018; Du et al., 2018). New pavement materials and methods to reinforce their structure
86 have also been assessed using FEM, and it has been demonstrated that such modifiers as
87 crumb rubber, fibers, and stabilized base layers can make a significant contribution to
88 rutting resistance and structural performance (Saberian et al., 2019; Wang and Wang,
89 2024). Other mechanisms of environmental and moisture-associated damage have been
90 demonstrated to increase rutting with lack of appropriate consideration in numerical
91 models (Wang et al., 2019; Hassani et al., 2020).

The new research directions show that there is a transition to high-fidelity FEM simulations that are combined with multiscale modeling, Digital Twin ideas, and data-driven methods to enhance prediction quality and provide proactive pavement management (VanDerHorn & Mahadevan, 2021; Yao et al., 2023). FEM with Digital Twin frameworks provide an opportunity to observe performance in real time, predict the remaining life, and plan the maintenance optimization (Dihan et al., 2024; Oditallah et al., 2025). Also, machine learning methods are also becoming actively considered as a means to complement FEM, as it provides less expensive calculations and improves the predictive quality of the model (Mazumder et al., 2023; Onaji et al., 2022). In this developing framework, the current research uses ABAQUS based FEM to purposefully explore the influence of pavement layer thickness on rutting depth of repeated loads in traffic with an object of making contributions on more credible rutting prediction and optimal flexible pavement design.

2. Materials and Methodology

This study employs a three-dimensional numerical modeling approach to investigate the structural response of a flexible pavement system under traffic loading. The finite element model was developed to simulate realistic pavement geometry, material behavior, and boundary conditions. The methodology includes detailed geometric modeling, material characterization, loading application, and meshing strategy to evaluate pavement performance.

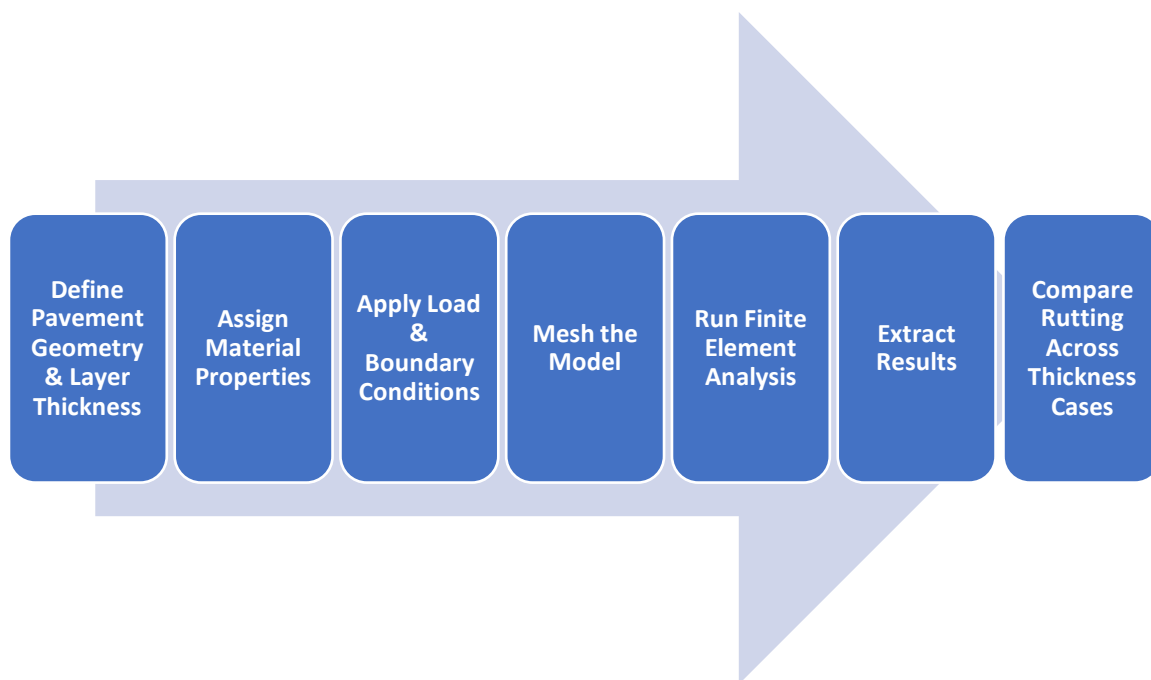
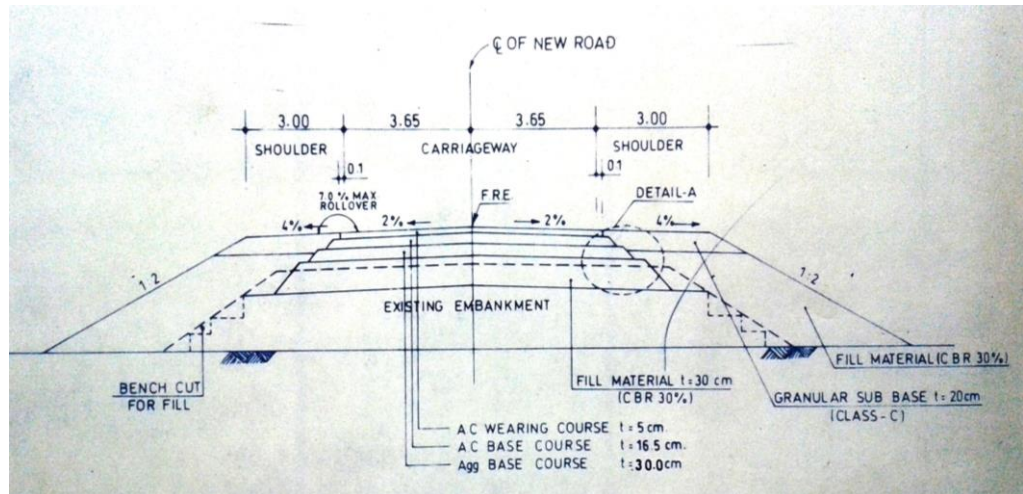


Figure 1 Methodology

2.1. Geometric Details

A multilayer flexible pavement system was modeled in ABAQUS with the following layers as shown in Figure 2:

1. Asphalt Concrete (AC) Wearing Course
2. Base Course (AC)
3. Base Course (Aggregate)
4. Subgrade (Fill Material)
5. Natural Subgrade



123

124

125

Figure 2 Typical Cross-section of Road

126

127

128

129

130

Multiple pavement configurations were analyzed by **varying the thickness** by +25% and -25% of Wearing Course and Base Course (AC), as shown in Table 1. So a total of nine configurations were analyzed.

Table 1 Geometric Properties

Layer	Original Thickness (mm)	Variable Thickness Cases (mm)
Wearing Course (AC)	50	62.5, 75, 37.5, 25,
Base Course (AC)	165	206.25, 247.5, 123.75, 82.5
Base Course (Aggregate)	300	Constant
Subgrade (Fill)	300	Constant
Natural Subgrade	1000	Constant

131

132

133

In ABAQUS software, the width and length of road were assigned 2000 mm each for each thickness case as shown Figure 3.

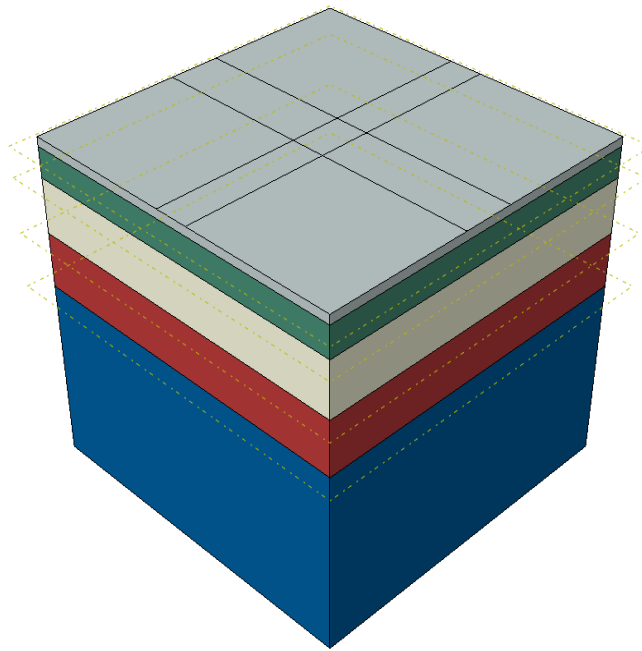


Figure 3 Assembly of Cross-section of Road

2.2. Materials

The pavement was modeled as a multilayer system, with each layer assigned realistic mechanical properties based on standard pavement engineering literature and empirical correlations. Table 2 summarizes the material parameters used in the finite element model.

Table 2: Material Properties

Layer	Young's Modulus E (MPa)	Poisson's Ratio ν	Density*10 ⁻⁹ (kN/mm ³)
Wearing Course (AC)	2758	0.25	2.4
Base Course	2413	0.20	2.3
Subbase	1379	0.30	2.2
Subgrade (Fill Material)	69	0.40	1.8
Natural Subgrade	34	0.45	1.6

The asphalt concrete (AC) layer was modeled as a linear elastic material for simplification, while the granular layers (base and subbase) and subgrade soils were modeled using an elastoplastic constitutive model to capture permanent deformation under repeated loading. A uniform foundation stiffness of 0.03 N/mm was applied at the bottom boundary to simulate the underlying soil support.

2.3. Loading, boundary conditions and interactions

A static dual-tire axle load of 80 kN was applied, representing a standard single axle with two tires. Each tire carried a load of 40 kN. The tire contact pressure was set to 827 kPa based on standard truck tire inflation pressures. The contact area for each tire was calculated as:

$$Contact\ Area = \frac{Load\ per\ Tire}{Tire\ Pressure} = \frac{40\ kN}{827\ kPa} \approx 0.0484\ m^2$$

The resulting applied pressure on each tire patch was:

$$P = \frac{40 \text{ kN}}{0.0484 \text{ m}^2} \approx 0.8333 \text{ MPa}$$

Thus, the total pressure applied by both tires was 1.66 MPa. The load was applied as a uniformly distributed pressure over rectangular contact patches aligned along the wheel path.

Boundary Conditions:

- The bottom of the model was fully fixed (encastre).
- The lateral sides were constrained in the horizontal direction to prevent lateral movement.
- A vertical foundation stiffness of 0.03 N/mm³ was applied at the base to simulate subgrade support.

2.4. Meshing

The pavement model was discretized with a structured hexahedral mesh. To create consistency and computational efficiency, a global mesh size was used of 100 mm being applied to each and every layer. Mesh sensitivity analysis established that this element size offered a trade-off between the accuracy of the results and the time of simulation.

3. Results

The output of the finite element analysis is performed to examine the impact of pavement layer thickness on the performance of rutting. The findings are the vertical movement (rut depth) and stress distribution and strain concentration among various pavement arrangements.

3.1. Deformation Distribution

The deformation contours extracted from ABAQUS provide insight into the mechanical response.

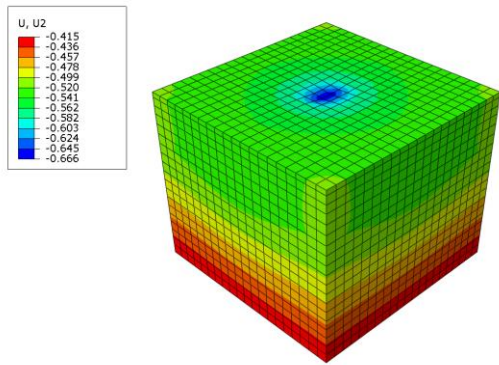


Figure 4 Deformation Contour (U2) for Original Configuration

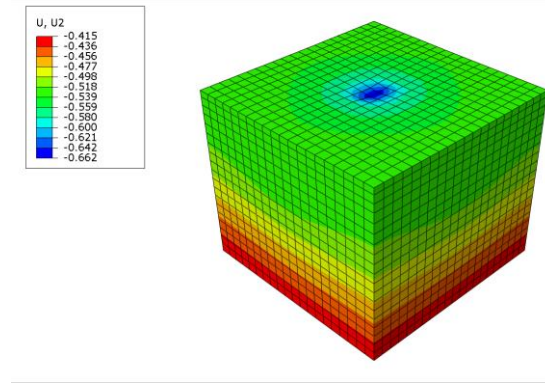


Figure 5 Deformation Contour for (X1)

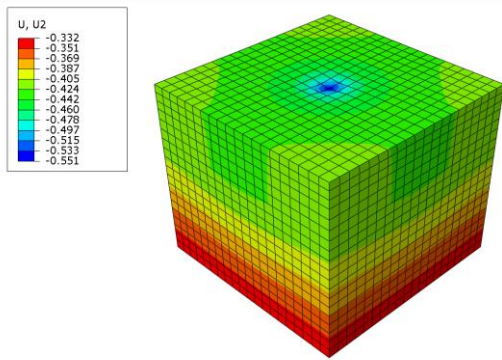


Figure 6 Deformation Contour for (X3)

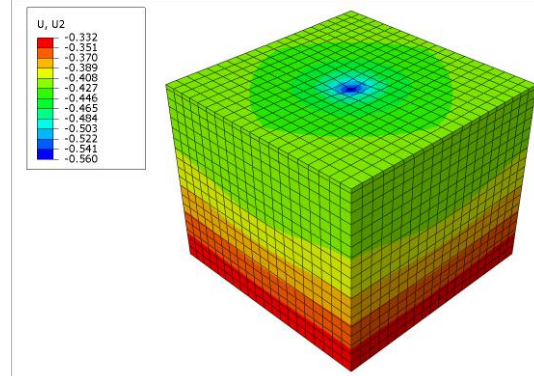


Figure 7 Deformation Contour for (X3)

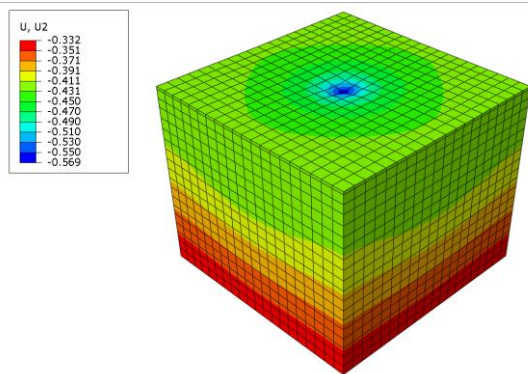


Figure 8 Deformation Contour for (X4)

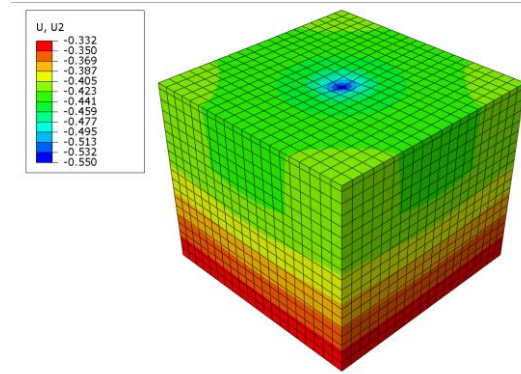


Figure 9 Deformation Contour for (X5)

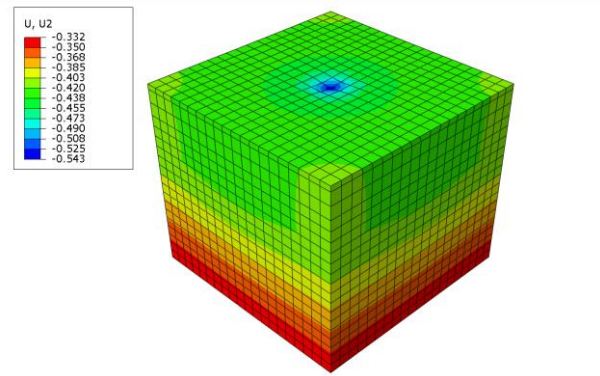


Figure 10 Deformation Contour for (X6)

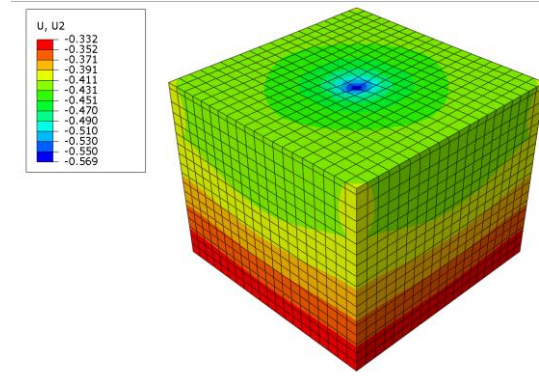


Figure 11 Deformation Contour for (X7)

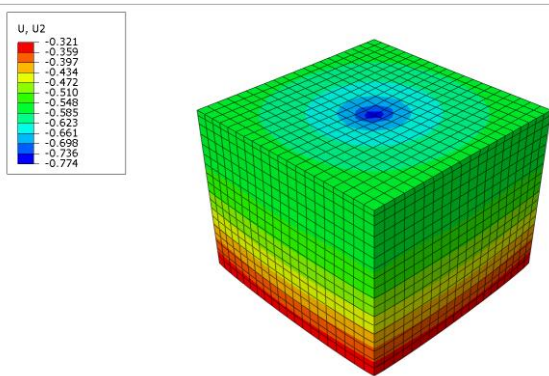


Figure 12 Deformation Contour for (X8)

The deformation contour plots above Figure 4 – Figure 12 show the compressive (U2) strain profiles of all pavement configurations that have been considered using the initial model through case X1 to X8. These images always emphasize that the depth of the layer plays a vital role in the level of strain reduction and distribution since the thicker parts of the layer demonstrate lower strain levels, especially in the subgrade and asphalt layers. The fact that these figures are a support to the quantitative rutting results to offer a mechanistic explanation of the deformation behavior that was observed in each of the design variants.

3.2. Rutting Depth Analysis

The total rutting depth was calculated as the sum of permanent vertical displacements accumulated in each pavement layer under repeated loading. The rut depth R for a given layer i is expressed as:

$$R_i = \varepsilon_{v,i} \cdot d_i$$

where:

- $\varepsilon_{v,i}$ = vertical strain in layer i
- d_i = thickness of layer i

The total rutting depth R_{total} is then:

$$R_{total} = \sum_{i=1}^n R_i = \sum_{i=1}^n (\varepsilon_{v,i} \cdot d_i)$$

181
182
183
184
185
186
187
188
189
190

191
192
193
194
195
196
197
198
199
200
201
202

In Table 3, values from X1 to X4 shows variable thickness in the Wearing Course by +25% and -25% while from X5-X6 shows variable thickness in the Base Course (AC) by +25% and -25%. Table 4 summarizes the calculated rutting depths for all pavement configurations, including variations in wearing course (AC) and base course thicknesses.

Table 3 Varying Thicknesses by +25% and -25% (mm)

Varying thickness by +25% and -25%		Wearing Course (AC)	Base Course (AC)	Base Course (Aggregate)	Subgrade (Fill Material)	Subgrade (Natural)	Total thickness
	Original	50	165	300	300	1000	1815
Varying the thickness of Wearing Course (AC)	X-1	62.5	165	300	300	1000	1827.5
	X-2	75	165	300	300	1000	1840
	X-3	37.5	165	300	300	1000	1802.5
	X-4	25	165	300	300	1000	1790
Varying the thickness of Base Course (AC)	X-5	50	206.25	300	300	1000	1856.25
	X-6	50	247.5	300	300	1000	1897.5
	X-7	50	123.75	300	300	1000	1773.75
	X-8	50	82.5	300	300	1000	1732.5

Table 4 Calculated Rutting Depths for Different Pavement Configurations (mm)

Layer	Original	X1	X2	X3	X4	X5	X6	X7	X8
Wearing Course (AC) Top	0.91	1.11	1.30	0.69	0.48	1.76	0.84	0.98	0.92
Base Coarse (AC) Top	1.37	0.79	1.42	1.52	1.68	2.52	1.50	0.90	0.11
Base Coarse Aggregate	1.96	1.64	1.93	1.429	1.93	0.45	1.94	3.08	0.84
Subgrade (Fill Material)	4.50	4.27	3.33	3.346	4.37	1.48	2.69	0.27	7.59
Subgrade (Natural)	8.98	8.44	4.37	4.160	6.88	6.39	5.09	8.48	10.979
Total Rutting Depth (mm)	17.72	16.26	12.35	11.145	15.34	12.61	12.05	13.71	20.439

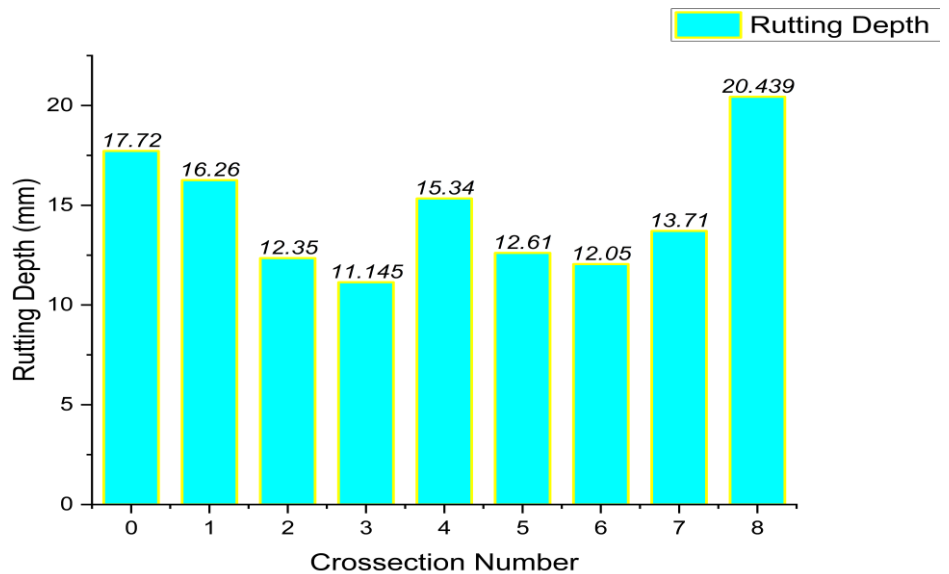


Figure 13: Cross-section configuration vs Rutting depth graph

4. Conclusions and Recommendations

Upon completion of an extensive three-dimensional analysis on finite element analysis conducted using ABAQUS software, this paper concludes that the layer thickness of pavements is a critical and quantifiable parameter in the control of rutting depth in the flexible pavement systems. The discussion clearly explained that adding the thickness of critical structural layers, especially the asphalt concrete wearing course and the granular base course, creates a significant decrease in the effect of permanent deformation through repeated traffic loading. Particularly, the geometry with a 37.5mm asphalt layer and with 165 mm base course produced the minimum rutting depth of 11.145 mm only, which indicates the relevance of proper structural depth in the allocation of loads and reduction of deformation in the subgrade.

The mechanistic contour plots further confirmed that increased thickness of the wearing course decreases the accumulation of rutting depth. These results also highly support the use of mechanistic-empirical design techniques in preference to the traditional empirical methods because the former make possible more finely, dependable, and cost-efficient pavement designs, which suit the particular traffic and material circumstances. Although the simplified linear elastic material assumptions and static loading used in this study were calculated-efficient because of its consistency, the trends remain consistent to form a sound basis of the practical design enhancement.

Future studies must combine more constitutive models (viscoelasticity of asphalt and plasticity of soils), dynamic and repeated load tests, and environmental effects (temperature and moisture) to improve predictive capability. Finally, this paper affirms that appropriate pavement layer thickness is a decisive factor in the strategic investment taking into consideration of the extending service life, the enhancement of ride quality, and variable structural performance even during the growing traffic pressure..

5. Patents

Author Contributions: The authors' contributions are as follows: Touqeer Ali Rind, Muhammad Faarid Shah, Mohammad Ahmad, Hafiz Ahmed Waqas, Shiraz Ahmed and Asad Wahab were responsible for the conceptualization, technical implementation, FEM Analysis, methodology, data collection, compilation, and validation and drafting of the paper.

Funding: This research received no external funding.

Acknowledgments: The authors would like to express their gratitude to the management of Ghulam Ishaq Khan Institute of Engineering Sciences and Technology, Topi, KPK, Pakistan, for their unwavering support and assistance throughout the duration of this study. .

Conflicts of Interest: The authors declare that there is no conflict of interest regarding this study and affirm that the work is original, without any form of plagiarism. All sources of information have been properly cited and acknowledged.

References

- [1] H. A. Waqas, M. Sahil, M. M. Khan, A. W. Anwar, M. U. Shah, and M. Usman, "Optimizing reinforcement strategies for robust beam-column joints in seismic resistant structures," *Arabian Journal for Science and Engineering*, 2024, doi: 10.1007/s13369-023-08591-1.
- [2] S. Mehran, A. Bahrami, H. A. Waqas, F. Amin, M. M. Khan, F. Iqbal, M. Fawad, and F. A. Najam, "Seismic performance evaluation of exterior reinforced concrete beam-column connections retrofitted with economical perforated steel haunches," *Results in Engineering*, vol. 22, p. 102179, 2024, doi: 10.1016/j.rineng.2024.102179.

- 258 [3] H. A. Waqas, A. Bahrami, M. Sahil, A. P. Khan, A. Ejaz, T. Shafique, Z. Tariq, S. Ahmad, and Y. A. Özkılıç, "Per-
259 formance prediction of hybrid bamboo-reinforced concrete beams using gene expression programming for sus-
260 tainable construction," *Materials*, vol. 16, no. 20, p. 6788, 2023, doi: 10.3390/ma16206788.
- 261 [4] F. Amin, H. A. Waqas, I. Ali, M. Waseem, M. Asif, K. A. Majid, and M. K. Leta, "Impact of carbon fiber-rein-
262 forced polymer sheets and bolt diameter on the seismic performance enhancement of steel beam-column joints,"
263 *Engineering Reports*, 2024, doi: 10.1002/eng2.13022.
- 264 [5] H. A. Waqas, M. Waseem, A. Riaz, M. Ilyas, M. Naveed, and H. Seitz, "Influence of haunch geometry and addi-
265 tional steel reinforcement on load carrying capacity of reinforced concrete box culvert," *Materials*, vol. 16, no. 4,
266 p. 1409, 2023, doi: 10.3390/ma16041409.
- 267 [6] Y. Du, J. Chen, Z. Han, and W. Liu, "A review on solutions for improving rutting resistance of asphalt pavement
268 and test methods," *Construction and Building Materials*, vol. 168, pp. 893–905, 2018, doi:
269 10.1016/j.conbuildmat.2018.02.151.
- 270 [7] A. Hassani, M. Taghipoor, and M. Karimi, "A state of the art of semi-flexible pavements: Introduction, design,
271 and performance," *Construction and Building Materials*, vol. 253, p. 119196, 2020, doi:
272 10.1016/j.conbuildmat.2020.119196.
- 273 [8] X. Luo, F. Gu, M. Ling, and R. Lytton, "Review of mechanistic-empirical modeling of top-down cracking in as-
274 phalt pavements," *Construction and Building Materials*, 2018, doi: 10.1016/j.conbuildmat.2018.10.005.
- 275 [9] A. Nasr, E. Kjellström, Í. Björnsson, D. Honfi, O. Ivanov, and J. Johansson, "Bridges in a changing climate: A
276 study of the potential impacts of climate change on bridges and their possible adaptations," *Structure and Infra-
277 structure Engineering*, vol. 16, no. 6, pp. 738–749, 2019, doi: 10.1080/15732479.2019.1670215.
- 278 [10] M. Oditallah, M. Alam, E. Palaneeswaran, and S. Ranjha, "Integration of pavement finite element simulation
279 with digital twin: Current practices, emerging trends, and future enablers," *Journal of Information Technology in
280 Construction*, vol. 30, pp. 544–569, 2025, doi: 10.36680/j.itcon.2025.023.
- 281 [11] W. Wang and L. Wang, "Review on design, characterization, and prediction of performance for asphalt materi-
282 als and asphalt pavement using multi-scale numerical simulation," *Materials*, vol. 17, 2024, doi:
283 10.3390/ma17040778.
- 284 [12] A. Singh and J. Sahoo, "Rutting prediction models for flexible pavement structures: A review of historical and
285 recent developments," *Journal of Traffic and Transportation Engineering*, vol. 8, no. 3, pp. 315–338, 2021, doi:
286 10.1016/j.jtte.2021.04.003.
- 287 [13] A. Duarte, N. Silvestre, J. de Brito, and E. Júlio, "Computational modelling of the cyclic behaviour of short rub-
288 berized concrete-filled steel tubes," *Engineering Structures*, 2021, doi: 10.1016/j.engstruct.2021.113188.
- 289 [14] E. VanDerHorn and S. Mahadevan, "Digital twin: Generalization, characterization, and implementation," *Deci-
290 sion Support Systems*, vol. 145, p. 113524, 2021, doi: 10.1016/j.dss.2021.113524.
- 291 [15] S. Su, R. Y. Zhong, Y. Jiang, J. Song, Y. Fu, and H. Cao, "Digital twin and its potential applications in construc-
292 tion industry: State-of-the-art review and a conceptual framework," *Advanced Engineering Informatics*, vol. 57, p.
293 102030, 2023, doi: 10.1016/j.aei.2023.102030.
- 294 [16] Md. S. Dihan *et al.*, "Digital twin: Data exploration, architecture, implementation and future," *Heliyon*, vol. 10,
295 2024, doi: 10.1016/j.heliyon.2024.e26503.
- 296 [17] J. Yao, Y. Yang, X.-C. Wang, and X. Zhang, "Systematic review of digital twin technology and applications," *Vis-
297 ual Computing for Industry, Biomedicine, and Art*, vol. 6, 2023, doi: 10.1186/s42492-023-00137-4.
- 298 [18] A. Alnedawi, K. Nepal, R. Al-Ameri, and M. Alabdullah, "Effect of vertical stress rest period on deformation
299 behaviour of unbound granular materials: Experimental and numerical investigations," *Journal of Rock Mechanics
300 and Geotechnical Engineering*, 2019, doi: 10.1016/j.jrmge.2018.05.004.

- 301 [19] M. Elseifi, J. Baek, and N. Dhakal, "Review of modelling crack initiation and propagation in flexible pavements
302 using the finite element method," *International Journal of Pavement Engineering*, vol. 19, no. 3, pp. 251–263, 2018,
303 doi: 10.1080/10298436.2017.1345555.
- 304 [20] W. Wang, L. Wang, H. Xiong, and R. Luo, "A review and perspective for research on moisture damage in as-
305 phalt pavement induced by dynamic pore water pressure," *Construction and Building Materials*, 2019, doi:
306 10.1016/j.conbuildmat.2019.01.167.
- 307 [21] M. Saberian, J. Li, and S. Setunge, "Evaluation of permanent deformation of a new pavement base and subbase
308 containing unbound granular materials, crumb rubber and crushed glass," *Journal of Cleaner Production*, 2019,
309 doi: 10.1016/j.jclepro.2019.05.100.
- 310 [22] X. Luo, F. Gu, Y. Zhang, R. Lytton, and D. Zollinger, "Mechanistic–empirical models for better consideration of
311 subgrade and unbound layers influence on pavement performance," *Transportation Geotechnics*, vol. 13, pp. 52–
312 68, 2017, doi: 10.1016/j.trgeo.2017.06.002.
- 313 [23] S. Benakli, Y. Bouafia, M. Oudjène, R. Boissiere, and A. Khelil, "A simplified and fast computational finite ele-
314 ment model for the nonlinear load–displacement behaviour of reinforced concrete structures," *Composite Struc-
315 tures*, 2018, doi: 10.1016/j.compstruct.2018.03.070.
- 316 [24] A. Mazumder *et al.*, "Towards next generation digital twin in robotics: Trends, scopes, challenges, and future,"
317 *Heliyon*, vol. 9, 2023, doi: 10.1016/j.heliyon.2023.e13359.
- 318 [25] I. Onaji, D. Tiwari, P. Soulatiantork, B. Song, and A. Tiwari, "Digital twin in manufacturing: Conceptual frame-
319 work and case studies," *International Journal of Computer Integrated Manufacturing*, vol. 35, no. 9, pp. 831–858,
320 2022, doi: 10.1080/0951192X.2022.2027014.
- 321